NeuroImage 66 (2013) 151–160

Contents lists available at SciVerse ScienceDirect

NeuroImage

journal homepage: www.elsevier.com/locate/ynimg

Identification of reproducible individualized targets for treatment of depression with TMS based on intrinsic connectivity

Michael D. Fox [a,b,c,*], Hesheng Liu [c], Alvaro Pascual-Leone [b,d]

[a] Partners Neurology, Massachusetts General Hospital, Brigham and Women's Hospital, Harvard Medical School, Boston, MA, USA
[b] Berenson-Allen Center for Noninvasive Brain Stimulation, Beth Israel Deaconess Medical Center and Harvard Medical School, Boston, MA, USA
[c] Athinoula A. Martinos Center for Biomedical Imaging, Harvard Medical School, Boston, MA, USA
[d] Institut Guttmann, Hospital de Neurorehabilitació, Universitat Autònoma de Barcelona, Barcelona, Spain

ARTICLE INFO

Article history:
Accepted 31 October 2012
Available online 7 November 2012

Keywords:
Transcranial magnetic stimulation
TMS
Intrinsic connectivity
Resting state functional connectivity
MRI
Subgenual
Dorsolateral prefrontal cortex
Depression
Individual differences
Variability
Seed map

ABSTRACT

Transcranial magnetic stimulation (TMS) to the left dorsolateral prefrontal cortex (DLPFC) is used clinically for the treatment of depression however outcomes vary greatly between patients. We have shown that average clinical efficacy of different left DLPFC TMS sites is related to intrinsic functional connectivity with remote regions including the subgenual cingulate and suggested that functional connectivity with these remote regions might be used to identify optimized left DLPFC targets for TMS. However it remains unclear if and how this connectivity-based targeting approach should be applied at the single-subject level to potentially individualize therapy to specific patients. In this article we show that individual differences in DLPFC connectivity are large, reproducible across sessions, and can be used to generate individualized DLPFC TMS targets that may prove clinically superior to those selected on the basis of group-average connectivity. Factors likely to improve individualized targeting including the use of seed maps and the focality of stimulation are investigated and discussed. The techniques presented here may be applicable to individualized targeting of focal brain stimulation across a range of diseases and stimulation modalities and can be experimentally tested in clinical trials.

Introduction

Repetitive transcranial magnetic stimulation (rTMS) is a non-invasive brain stimulation technique that is showing utility in the treatment of a variety of neurological and psychiatric disorders (Burt et al., 2002; Fregni and Pascual-Leone, 2007; Hallett, 2007). Its most common use involves high-frequency stimulation to the left dorsal lateral prefrontal cortex (DLPFC) for the treatment of depression (George et al., 1995; O'Reardon et al., 2007; Padberg and George, 2009; Pascual-Leone et al., 1996). In the US, the Neuronetics® device and Neurostar protocol are approved by the Food and Drug Administration for some patients with medication-resistant depression. However, the clinical utility of rTMS remains limited by large heterogeneity in clinical response.

One factor known to contribute to this response heterogeneity is differences in the site of stimulation in the left DLPFC (Ahdab et al., 2010; Fitzgerald et al., 2009; Herbsman et al., 2009; Herwig et al., 2001; Padberg and George, 2009). The targeting technique routinely employed in clinical practice, and followed by the FDA approved protocol, is to center the TMS coil at a point 5 cm anterior to the motor cortex measured along the curvature of the scalp. This approach identifies different stimulation sites in different subjects (Ahdab et al., 2010; Herwig et al., 2001) and some sites appear to be more effective than others at producing an antidepressant response (Fitzgerald et al., 2009; Herbsman et al., 2009; Padberg and George, 2009; Paillère Martinot et al., 2010). In an effort to understand why some sites are more effective, we recently used intrinsic (resting state) fMRI to identify differences in functional connectivity between effective and less effective DLPFC stimulation sites at the population level (Fox et al., 2012a). Significant differences in connectivity were seen in a variety of cortical and limbic regions including the subgenual cingulate, a region repeatedly implicated in antidepressant response to a variety of treatment modalities (Drevets et al., 2008; Mayberg, 2009; Mayberg et al., 2005). Specifically, left DLPFC sites which when targeted with TMS leads to greater antidepressant effects, showed a stronger negative correlation (anticorrelation) with the subgenual. Based on these findings, we proposed a connectivity-based targeting strategy for TMS and used this technique to identify theoretically optimal TMS target coordinates in the left DLPFC at the population level (Fox et al., 2012a).

An important advantage of this connectivity-based targeting strategy is that it might be scaled from the population level down to the level of single subjects to tailor treatment to individual patients. The DLPFC varies greatly between individuals on a histological basis (Rajkowska and Goldman-Rakic, 1995) thus the population-average

* Corresponding author at: Partners Neurology, Massachusetts General Hospital, Brigham and Women's Hospital, Harvard Medical School, Boston, MA, USA.
E-mail address: foxmdphd@gmail.com (M.D. Fox).

1053-8119/$ – see front matter © 2012 Elsevier Inc. All rights reserved.
http://dx.doi.org/10.1016/j.neuroimage.2012.10.082

TMS coordinates might be suboptimal for many patients. However individualized targeting will be associated with an inherent worsening of signal to noise that could overwhelm any benefit of accounting for individual differences. For example, targeting a population-average focus of hypometabolism in the left DLPFC with TMS appears superior to the standard 5 cm technique (Fitzgerald et al., 2009), however three separate studies aiming to target individualized foci of hypometabolism failed to provide clinical benefit (Garcia-Toro et al., 2006; Herwig et al., 2003a; Paillère Martinot et al., 2010). In fMRI, the subgenual is a region with poor signal to noise ratio (Ojemann et al., 1997) and intrinsic anticorrelations may be less reproducible than positive correlations (Shehzad et al., 2009). It therefore remains unclear if connectivity-based targeting can identify individualized TMS sites in the DLPFC that are sufficiently robust and reproducible to potentially be used in the treatment of depression.

In the current article we show that individual differences in DLPFC connectivity are large, reproducible across scanning sessions, and can be translated into individualized TMS targets on the cortical surface. Further, we identify factors likely to improve individualized targeting such as the use of seed maps and the focality of stimulation.

Methods

Subjects and data collection

This study utilized three independent datasets, each of which was used for a particular set of analyses (Fig. 1). Datasets 1 and 2 have been used in prior published articles (Fox et al., 2012a; Van Dijk et al., 2012; Yeo et al., 2011) and were not collected specifically for the present paper. However these prior articles investigated different experimental questions than those investigated in the current article and no part of the present report overlaps with prior published findings. Dataset 3 was collected specifically for the present investigation.

1) The first dataset consisted of 98 healthy right-handed subjects (48 male, age 22 ± 3.2 years (mean ± SD)) and was used for initial analyses of individual differences and as an independent cohort to construct group-level functional connectivity maps. This was a subset of subjects from a prior analysis of resting state functional connectivity across 1000 subjects (Yeo et al., 2011) and the same cohort used in our recent paper on group differences in connectivity between different left DLPFC TMS sites (Fox et al., 2012a). Experiments were conducted with the written consent of each subject and approved by the Partners' Institutional Review Board. Imaging was performed on a 3 T Siemens whole body MRI System with a phased array head coil. Each subject completed two 6.2 min long (124 frames) resting state fMRI scans (TR = 3000 ms, TE = 30 ms, FA = 85°, 3 × 3 × 3 mm voxels, FOV = 216, 47 axial slices with interleaved acquisition and no gap). During scanning, participants were instructed to keep their eyes open and remain still. Structural data included a high-resolution multi-echo T1-weighted magnetization-prepared gradient echo image (TR = 2200 ms, TI = 1100 ms, TE = 1.54 ms for image 1 to 7.01 ms for image 4, FA = 7°, 1.2 × 1.2 × 1.2 mm voxels, FOV = 230)(van der Kouwe et al., 2008).
2) The second dataset consisted of 42 healthy right-handed subjects (16 male, age 20 ± 2.0 years (mean ± SD)) scanned during two different MRI sessions separated by 68 ± 54 days (mean ± SD), range 2–230 days, and was used to assess reproducibility of individual differences across scanning sessions. This is also a subset of subjects used in a prior analysis of resting state functional connectivity across 1000 subjects (Yeo et al., 2011) and has been previously used to examine the reproducibility of subject head motion (Van Dijk et al., 2012). The protocol was identical to the above with the exception that all subjects completed two scanning sessions on two separate days.
3) The third and final dataset consisted of 2 patients with medication-resistant depression (both female, one right and one left-handed, age 53 and 55, Hamilton Depression Rating Scale scores of 16 and 29) scanned during two different MRI sessions separated by 2–3 weeks, and was used to demonstrate reproducible individual differences in connectivity similar to our larger cohort of normal subjects. Patients had Major Depressive Disorder diagnosed by a psychiatrist according to the criteria of the DSM-4 and were recruited from those presenting to Beth Israel Deaconess Medical Center (BIDMC) for therapeutic TMS. Experiments were conducted with the written consent of each patient and approved by the Institutional Review Board at BIDMC. In between the two MRI scans patients received therapeutic rTMS to the left DLPFC following the FDA-approved Neurostar protocol (Neuronetics). However potential changes in connectivity induced

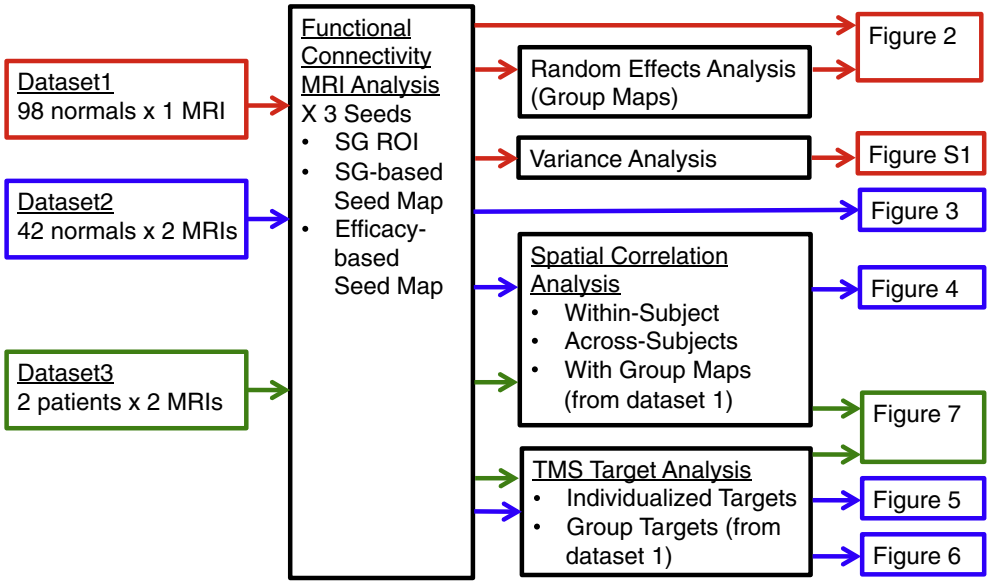

Fig. 1. Outline of datasets, analyses, and figures used in the current article. MRI data from dataset 1 (red), dataset 2 (blue), and dataset 3 (green) were run through different analyses (black boxes) and the results presented in several figures (right). The color of the box around each figure indicates the dataset used to generate that figure. SG = subgenual.

by TMS were not assessed nor part of the current experiment. MR imaging was conducted using a GE 3 T MRI routinely used for clinical research. High-resolution T1-weighted structural images were acquired via a 3D modified driven-equilibrium Fourier transform (MDEFT) prepared fast Spoiled Gradient Echo (SPGR) sequence ($0.94\times0.94\times1$ mm resolution, TE 2.9 ms, flip angle 15°). This was followed by four resting state fMRI BOLD runs each 6 min 37 s (124 frames) in duration (TR 3.2 s, TE 30, flip angle 90°, $3.75\times3.75\times3$ mm resolution). BOLD imaging employed fat-saturation rather than the scanner default spatial spectral excitation because it minimized signal loss in the ventral medial prefrontal cortex. Array Spatial Sensitivity Encoding Technique (ASSET), a vendor version of parallel imaging, with acceleration factor 2 was used to minimize geometric distortion of the BOLD sensitive images. During the resting state fMRI scans the subjects were asked to lay still and stare at a fixation cross.

A priori defined regions of interest

Two regions of interest (ROI) were defined a priori for use in the present analysis, one in the subgenual cingulate cortex and another in the left DLPFC. Details regarding the creation of these ROIs have been presented previously (Fox et al., 2012a). Briefly, the subgenual ROI was constructed by placing a 10 mm radius sphere at MNI coordinates (6, 16, −10), masked to include only sampled gray matter voxels. These subgenual coordinates were chosen based on prior studies where a reduction in subgenual activity was associated with antidepressant response across a wide range of treatment modalities (Drevets et al., 2002; Kito et al., 2008, 2011; Mayberg et al., 2000, 2005; Nahas et al., 2007; Wu et al., 1999) (see Table 1 in Fox et al, 2012a).

A large ROI designed to cover what is generally considered the left DLPFC was constructed by centering 25 mm radius spheres on MNI coordinates at the center of Brodmann area (BA) 9 (−36, 39, 43), the center of BA46 (−44, 40, 29), and the average DLPFC site stimulated using the standard 5 cm targeting technique (−41, 16, 54). Spheres were summed and masked to include only sampled gray matter voxels. Coordinates for Brodmann regions (BA9 and 46) were based on Rajkowska and Goldman-Rakic (1995). However this paper reported only y and z coordinates so the x coordinate was determined from the coordinate in Talairach space on the cortical surface constrained by the y and z coordinates (Talairach and Tournoux, 1988). This complete set of Talairach coordinates was transformed into MNI space using tal2mni (http://imaging.mrc-cbu.cam. ac.uk/imaging/MniTalairach). Coordinates for the average 5 cm site were based on coordinates averaged from two prior TMS studies (Herbsman et al., 2009; Herwig et al., 2001).

Data processing

fMRI data were processed in accordance with the strategy of Fox et al. (2005) as implemented in Van Dijk et al. (2010). Briefly, the first four volumes of each run were discarded, slice-acquisition-dependent time shifts were compensated per volume using SPM2 (Wellcome Department of Cognitive Neurology, London, UK), and head motion was corrected using rigid body translation and rotation using FMRIB Software Library (Oxford, UK)(Jenkinson et al., 2002). Atlas registration was achieved by computing affine and nonlinear transforms connecting the first volume of the functional run using SPM2, with a T1 EPI template in the Montreal Neurological Institute (MNI) atlas space. Data were resampled to 2-mm isotropic voxels and spatially smoothed using a 6-mm full-width half-maximum (FWHM) Gaussian kernel. The data underwent further preprocessing specific to functional connectivity analysis, including low-pass temporal filtering ($f<0.08$ Hz), head-motion regression, whole-brain signal regression, and ventricular and white matter signal regression using custom-designed in-house software (Fox et al., 2005; Van Dijk et al., 2010).

Three "seed regions" were used in the present functional connectivity analysis, all taken from a prior study of DLPF and subgenual functional connectivity (Fig. 2) (Fox et al., 2012a). The first seed region was simply the small subgenual ROI as defined above (subgenual ROI). The second seed was the entire subgenual functional connectivity map previously generated using random effects analysis across 98 subjects (SG-based seed map). The third seed was the entire functional connectivity map of effective vs ineffective DLPF stimulation sites, previously generated using a paired t-test across 98 normal subjects (efficacy-based seed map). The latter two "seed maps" cover the entire brain with the exception of the left DLPFC which was omitted to avoid biasing of results in this region. Time courses were extracted from each seed region or seed map by computing a weighted average of all voxels within the seed at each time point. Voxel weights for the seed maps were continuous variables and could be positive or negative. The Pearson's correlation coefficient was computed between this extracted time course and that of all other voxels. Fisher's r-to-z transformation was used to convert correlation maps into z maps.

To determine the similarity between two functional connectivity maps, a spatial correlation coefficient was computed across voxels (Fox et al., 2006). To normalize the distributions for statistical comparison, spatial correlation values were converted using Fisher's r-to-z transform. These values are listed in the text as z(r). After averaging and statistical comparison, these values were transformed back to r values using the inverse Fisher transform and the percentage variance accounted for in each comparison was computed as r^2 (Supplementary Table 1). Although intuitive, the spatial correlation coefficient may miss some differences when comparing two maps (i.e. scalar offsets or differences in magnitude) so we also compared maps using a spatial eta coefficient (Cohen et al., 2008). Results were nearly identical using these two metrics of similarity, so only the results using the spatial correlation coefficient are presented here.

To create a set of potential TMS target sites, we first identified all voxels on the surface of the standard MNI152 brain template based on gray scale intensity (21,415 nodes). These voxels were then down-sampled to 4 mm resolution (4045 nodes) and masked to include only those voxels in the left DLPFC (163 nodes). The center coordinates for each of these surface nodes were identified resulting in a set of 163 potential TMS target coordinates in the left DLPFC separated from each other by at least 3 mm in all directions (Supplementary Fig. 1A). Using in-house software, we generated spheres of varying radii centered on these node coordinates to reflect varying focality of different potential cortical stimulation techniques (Supplementary Figs. 1B,C). Spheres ranged in size from 1 to 30 mm in radius for analysis purposes, but this is not meant to suggest that commercially available TMS coils are capable of focally stimulating a 1 mm area. Each sphere was masked to exclude voxels outside the brain. For most analyses these spheres were of uniform intensity to simplify the analysis, interpretation, and comparison across sphere sizes. However, for one analysis surface spheres were constructed to have a decreasing intensity with an increased distance from the sphere center to more accurately model a true TMS coil (Supplementary Fig. 2). It is important to note that accurately modeling the volume of TMS-induced changes in neuronal activity is complicated and depends on the specific stimulation coil, intensity, coil orientation, underlying anatomy, and assumed neuronal depolarization function (Deng et al., 2012; Wagner et al., 2007). Such advanced modeling is beyond the scope of the present investigation. To generate a rough approximation, we created a series of concentric spheres of radius 2, 4, 7, 9, and 12 mm (12 mm cone) chosen to match the linear decay of metabolic changes seen in animal TMS experiments (Valero-Cabre et al., 2005). When compared to a model of the induced electric field of a standard figure-eight TMS coil (Pascual-Leone et al., 2002; Thielscher and Kammer, 2004), the distance of 12 mm corresponds

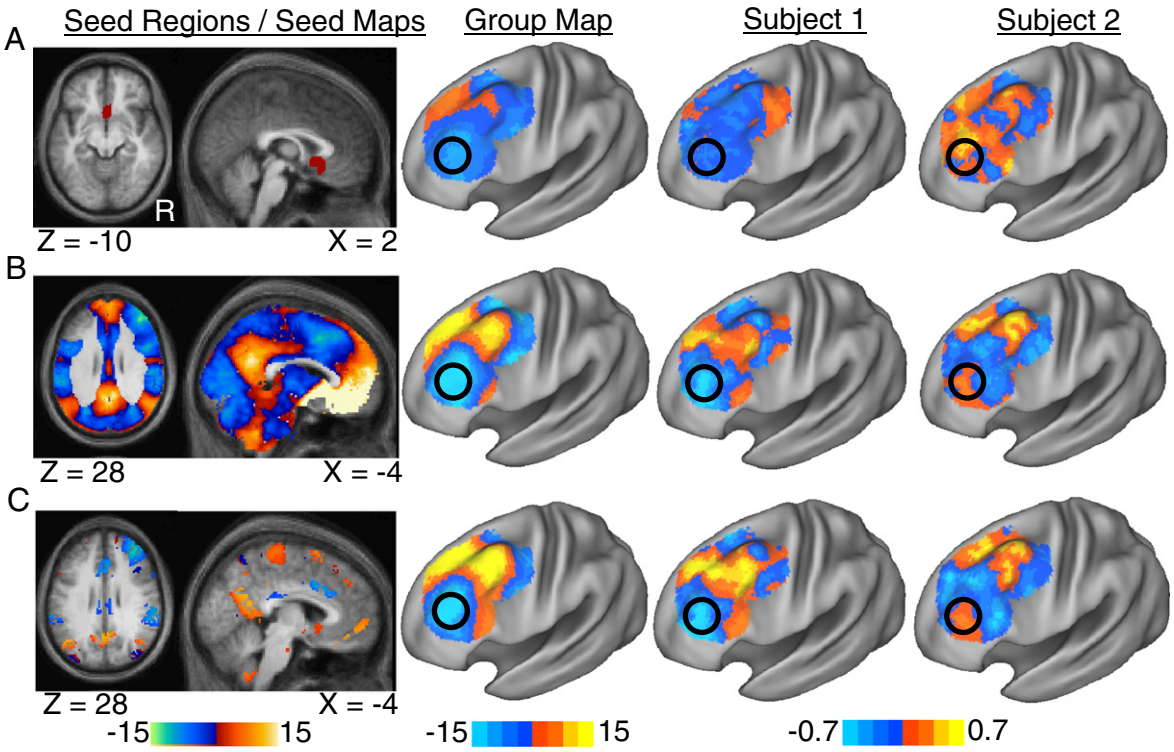

Fig. 2. Identification of connectivity-based TMS targets in the left dorsal lateral prefrontal cortex (DLPFC) at the group and single subject level. Resting state functional connectivity maps are shown for the population (group) and two individual subjects (Subjects 1 and 2) for a seed region in the subgenual cingulate (A) a seed map based on subgenual connectivity (B) and a seed map based on connectivity differences between effective and ineffective DLPFC TMS sites (C). Surface-based maps are masked to show only voxels in the left DLPFC. Black circles identify a potential stimulation site at the group level that is different between Subjects 1 and 2.

to a field intensity of around 75% of maximum (Supplementary Fig. 2). This seems appropriate given that this intensity is near the limit at which sub-threshold conditioning pulses produce a physiological effect in human paired-pulse experiments (Kujirai et al., 1993).

The optimal stimulation node for a given functional connectivity map and sphere size was identified by computing the average voxel value (Fisher z score) within each surface sphere then selecting the node with the most negative value. For our 12 mm cone model the varying ROI intensity was normalized to a mean of 1 and a weighted average was used to select the optimal ROI. Using this approach, optimal stimulation nodes were identified for each subject, day, sphere size, and functional connectivity map. For comparison, optimal stimulation nodes were also identified for each sphere size and seed region using the three group-level functional connectivity maps from the independent 98-subject cohort (dataset 1). To compare ROIs selected on the basis of individualized maps to those selected on the basis of the group map, the average voxel value (Fisher z score) within each ROI was computed using the single-subject functional connectivity data from the alternate day (i.e. the day not used to select the stimulation node). The superior targeting technique for a given subject is the one that identified the stimulation node with the more negative value in the independent dataset. The difference between individualized and group-based targeting as well as the effect of sphere size was determined using a two-way ANOVA and followed by paired t-tests for each sphere size and seed map.

It is important to note that this reproducibility analysis is not designed to determine if the same stimulation node will be identified in the same subject on two different days, but rather to determine if the stimulation node identified on one day still overlies an anticorrelated area on the second day. This analysis approach is less susceptible to random variation that might occur in a subject with multiple foci of anticorrelation.

All data processing, calculations, and thresholding were performed in volume space. For display purposes data were mapped to the cortical surface using CARET and the PALS atlas (Van Essen, 2005) using the average fiducial mapping option.

Results

Functional connectivity was computed with three seed regions/seed maps to identify candidate TMS targets in the left DLPFC (Fig. 2). Regardless of whether one used the small subgenual seed region (Fig. 2A), the full subgenual-based seed map (Fig. 2B), or the efficacy-based seed map (Fig. 2C), a clear anticorrelated area was identified at the group level (black circles). Peak MNI coordinates for these anticorrelations for the three group maps are (−42, 38, 34), (−42, 44, 26), and (−38, 44, 26) respectively. However, when examining the results from single subjects, pronounced heterogeneity was apparent. For example, as illustrated in Fig. 2, the ideal group-level stimulation target may suffice for Subject 1, but is far from the ideal target for Subject 2.

To obtain an estimate of the magnitude of these individual differences in functional connectivity, the standard deviation across subjects for every voxel in the left DLPFC was computed (Supplementary Fig. 3). For reference, this variance was compared to the standard deviation across all left DLPFC voxels within a subject. For the subgenual seed region, the variability across subjects was actually slightly larger than the variability across space within the DLPFC (0.192 vs 0.183 z(r)). Averaged across all three seed regions/maps, the variability across subjects was 0.241 while the variability across space was 0.285 z(r). This suggests that differences in DLPFC connectivity across subjects are of similar magnitude to differences in connectivity across space within the left DLPFC.

To determine if these individual differences were reproducible across time, DLPFC connectivity with the three seed regions/seed maps was computed in 42 subjects scanned on two separate days (Fig. 3). The functional connectivity maps for subject one on day

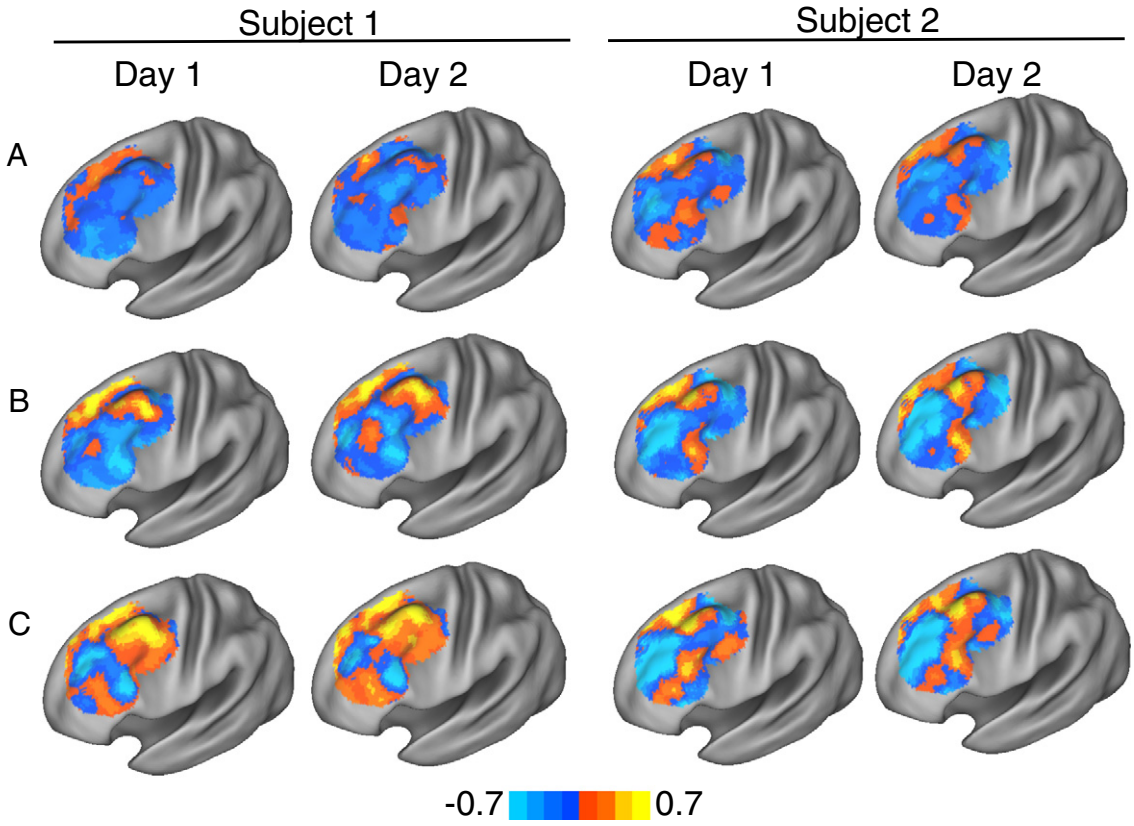

Fig. 3. Reproducibility of individual differences in dorsal lateral prefrontal cortex (DLPFC) connectivity across scanning sessions for two example subjects. Resting state functional connectivity maps are shown for two subjects (Subjects 1 and 2) scanned on two separate days (days 1 and 2) using a seed region in the subgenual cingulate (A) a subgenual-based seed map (B) and an efficacy-based seed map (C).

one appear similar to the maps from the same subject on day two, but very different from the maps of subject two. This qualitative impression was quantified by computing the similarity (spatial correlation) between DLPFC connectivity maps from the same subject on two separate days vs the similarity between maps from different subjects (Fig. 4, left). All three seed regions/maps showed significantly more consistency within a subject than between subjects including the subgenual seed region ($z(r) = 0.345$ vs 0.111, $P < 10^{-4}$), subgenual-based seed map ($z(r) = 1.22$ vs 0.537, $P < 10^{-17}$) and efficacy-based seed map ($z(r) = 1.32$ vs 0.567, $P < 10^{-21}$). These Fisher z values were transformed into r^2 values to estimate the percent variance in one map explained by another map and ranged from 1% ($z(r) = 0.11$) to 75% ($z(r) = 1.32$) (Supplementary Table 1). DLPFC connectivity remained reproducible within a subject even when comparing across our three different seed regions. Specifically, DLPFC connectivity within a subject with different seeds (and different sessions) was more similar than the same seed across different subjects ($z(r) = 0.618$ vs 0.396, $P < 10^{-6}$).

The above results attest to reproducibility of individual differences and indicate that subjects are more similar to themselves scanned on a different day than they are to other subjects. However, no one would propose targeting TMS in one subject based on connectivity results from another subject. A more pertinent comparison for determining the best way to target TMS is to compare single subject maps to that of the population (Fig. 4, right). Subjects were more similar to themselves scanned on a different day than they were to the population map for the subgenual-based seed map ($z(r) = 1.22$ vs 0.846, $P < 10^{-13}$) and efficacy-based seed map ($z(r) = 1.32$ vs 0.898, $P < 10^{-12}$) but not for the small subgenual seed region ($z(r) = 0.345$ vs 0.344, $P > 0.9$).

Importantly, not all seed regions performed equally well. Both the subgenual-based and efficacy-based seed maps were significantly more reproducible across days than the smaller subgenual seed region ($P < 10^{-16}$). In fact, connectivity with the subgenual-based seed map was a better predictor of connectivity with the small subgenual seed region on a separate day than connectivity with the subgenual seed region itself ($z(r) = 0.426$ vs 0.345, $P < 0.05$). This result held true even when the subgenual and the majority of the ventral medial prefrontal cortex were excluded from the subgenual-based seed map (Supplementary Fig. 4).

It is important to determine if these individual differences in DLPFC connectivity can actually be translated into individualized TMS targets constrained to the cortical surface. Further, it is important to determine if a TMS target selected on the basis of individualized functional connectivity has the potential to result in a better clinical outcome than a target selected on the basis of functional connectivity averaged across a large group. An example of our analysis approach for addressing these questions is shown for a single subject (Fig. 5). An optimal TMS target (6 mm sphere) for this subject was selected both on the basis of group-averaged connectivity (red box) and individualized connectivity from day one (blue box). The potential clinical utility of these targets was then tested using the independent functional connectivity results from that subject for day 2 (black box). Specifically, we determined which target corresponded to the more negatively correlated voxels in the independent dataset. For this subject and sphere size, individualized targeting selected a better (more negatively correlated) stimulation site than population-based targeting, which could lead to a better clinical response.

Similar analyses were conducted for all subjects using our three possible seed regions/maps with stimulation fields ranging in size from 1 mm radius to 30 mm radius (Fig. 6). Two-way ANOVAs were conducted for each seed region using targeting method and sphere size as factors. For each seed region/seed map there was a significant

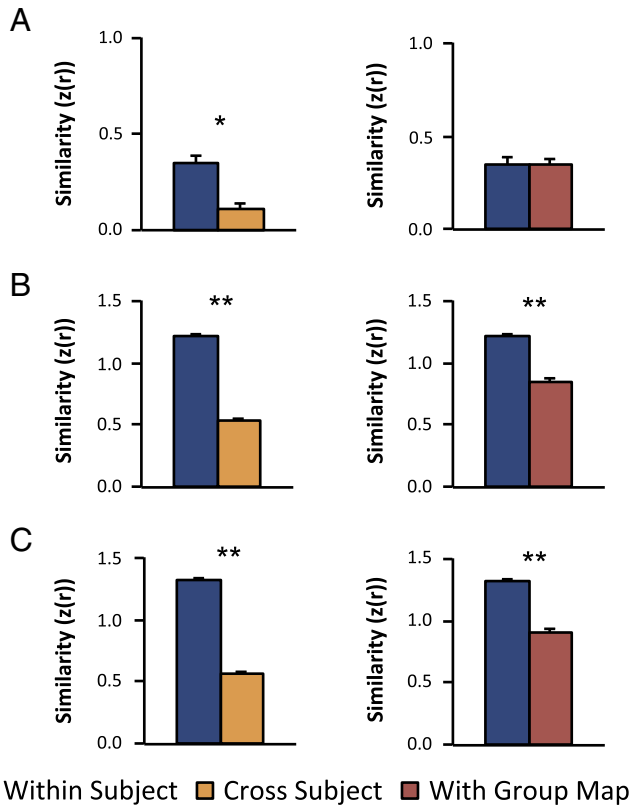

Fig. 4. Similarity of dorsal-lateral prefrontal cortex (DLPFC) functional connectivity within individual subjects scanned on two separate days compared to the similarity between different subjects or between individual subjects and the group average. Bar graphs show the similarity (spatial correlation) between functional connectivity maps in the left DLPFC for individual subjects compared to themselves scanned on a different day (blue) other subjects (orange) or the group map (red) for the small subgenual seed region (A), the subgenual-based seed map (B), and the efficacy-based seed map (C). * $P<10^{-4}$, **$P<10^{-12}$

difference between individualized and group-based targeting ($F=16.15$ to 37.99, $df=1$, $P<10^{-4}$), a significant difference between sphere sizes ($F=5.88$ to 209.56, $df=5$, $P<10^{-4}$), and a significant interaction between the two ($F=4.51$ to 5.04, $df=5$, $P<0.0005$). F values reflect the range across the three seed regions while P values reflect the least significant effect. Follow-up paired t-tests showed that individualized targeting identifies a better stimulation site (i.e. more anticorrelated node) than group-based targeting at several sphere sizes for each seed map (Fig. 6). The benefit of individualized targeting becomes more significant as the sphere size decreases and is more significant for the two seed maps compared to the smaller and noisier subgenual ROI. In fact, at the largest (30 mm) sphere size there was actually a significant benefit of using group-based over individualized targeting for the small subgenual seed region.

To obtain a rough approximation of the size of the stimulation field and potential benefit of individualized targeting for commercially available figure-eight TMS coils, we compared individualized to group-based targeting using a 12 mm radius cone-shaped field rather than a simple sphere (Fig. 6, column labeled cone). A two-way ANOVA using targeting method and seed region as factors revealed a significant difference between individualized and group-based targeting ($F=6.00$, $df=1$, $P<0.05$), a significant difference between seed regions ($F=238.4$, $df=2$, $P<10^{-15}$), but no significant interaction ($F=0.322$, $df=2$, $P=0.72$). Follow-up paired t-tests showed a significant benefit of individualized targeting for the subgenual-based seed map ($P<0.007$) and the efficacy-based seed map ($P<10^{-4}$) but not the small subgenual seed region ($P=0.12$).

Although normal subjects provide a large and useful dataset for methodological development and statistical testing, it is important to know if the methods have any utility in the population of interest, namely patients with medication-refractory depression presenting for brain stimulation. Repeating the above analyses on two such patients, results replicated the findings seen in the normal subjects. Results for the subgenual-based seed map are displayed here (Fig. 7) with the results for other seed regions and node coordinates for each patient tabulated in Supplementary Table 2. Both patients were more similar to themselves scanned on a different day than to the other

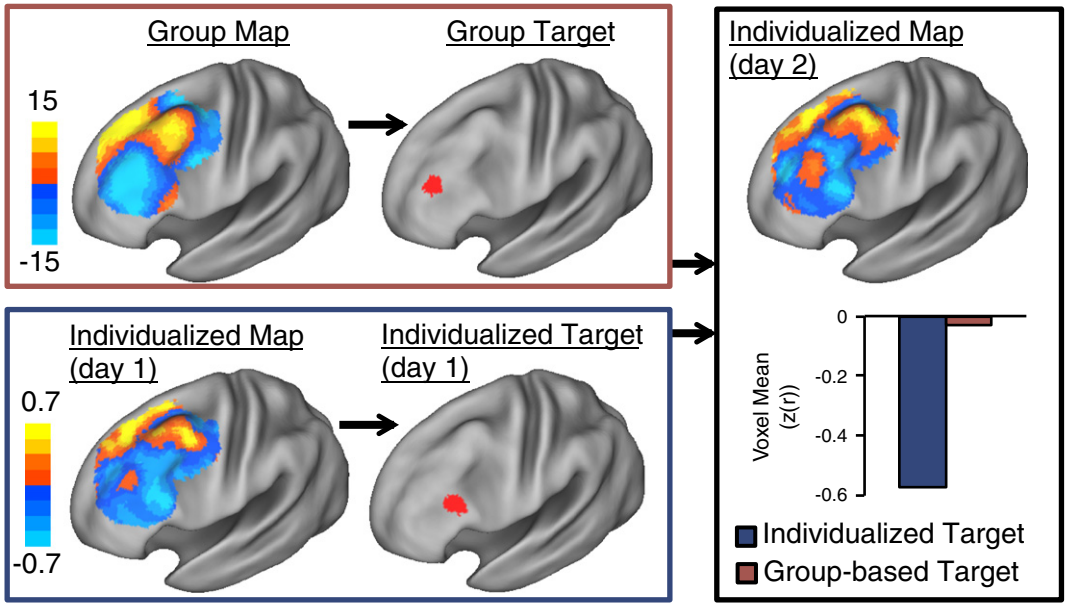

Fig. 5. Example of TMS targets identified based on group vs individualized functional connectivity for a single subject. Functional connectivity with the subgenual-based seed map was used to identify an optimal TMS target (i.e. strongest anticorrelation within a 6 mm sphere) in the left DLPFC based on the group map (red box) or individualized single-subject data from day 1 (blue box). The relative utility of these two targets was then tested using the independent single-subject fcMRI data from day 2 (black box). The average voxel value within the individualized target (blue bar) was compared with the average value within the group-based target (red bar). For this subject and sphere size, individualized targeting identifies a better anticorrelated node in the independent dataset than group-based targeting.

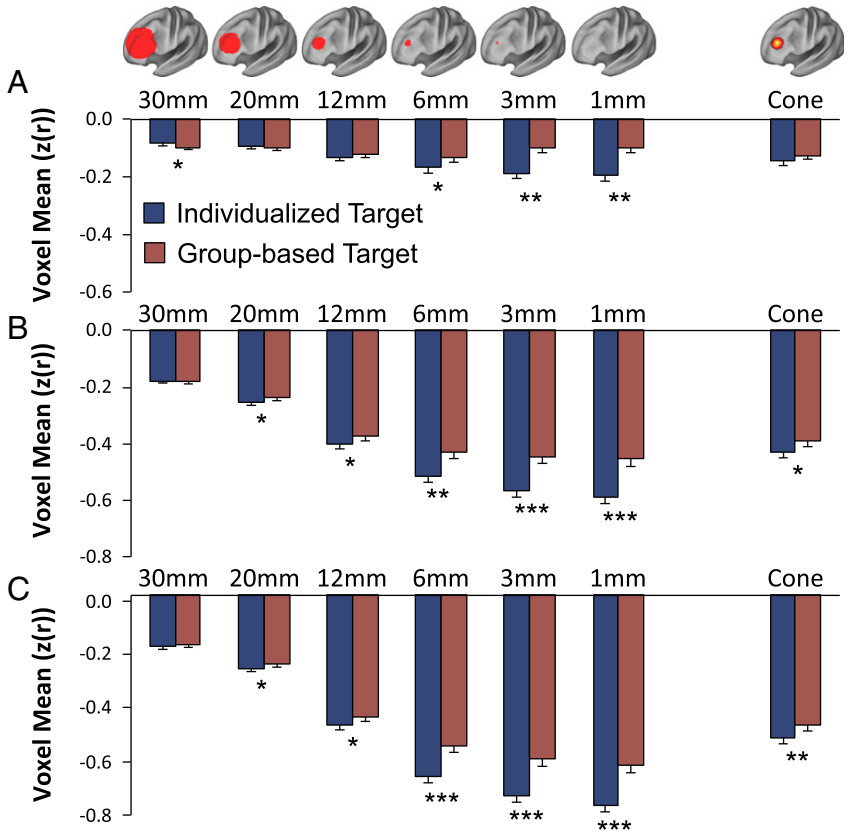

Fig. 6. The difference between individualized and population-based targeting of TMS varies depending on the modeled size of the stimulated tissue. Graphs show the average voxel value from day 2 within presumptive TMS targets of various sizes (spheres of radii 1–30 mm and a 12 mm cone) identified on the basis of either individualized functional connectivity from day 1 (blue bars) or the group map (red bars). Results are shown for the small subgenual ROI (A), the subgenual-based seed map (B), and the efficacy based seed map (C). Significant differences between individualized and population-based targeting are identified. * $P<0.05$, ** $P<0.0005$, *** $P<10^{-5}$.

patient for all three seed regions. Patients were also more similar to themselves than the group map for the subgenual-based and efficacy-based seed maps, but not for the small subgenual ROI. Using the 12 mm cone as our TMS field model, selecting a TMS site based on individualized connectivity identified a more anticorrelated node in the independent fMRI data than selecting the site based on group connectivity.

Discussion

There are several novel results in the present paper important for successful individualized targeting of TMS to the DLPFC based on functional connectivity. First, individual differences in DLPFC connectivity are large and reproducible across sessions. Second, TMS targets can be selected based on these individual differences and have the potential to be clinically superior to targets selected on the basis of a group map. Finally, individualized targeting might be improved through the use of a seed map over a seed region and becomes particularly advantageous when considering more focal stimulation.

Individualized targeting of TMS

The idea that one should target therapeutic TMS in depression based on individual differences in anatomy or function is not new. Further, it is widely recognized that the conventional 5 cm targeting technique is insufficient (Ahdab et al., 2010; Fitzgerald et al., 2009; Herbsman et al., 2009; Herwig et al., 2001; Padberg and George, 2009). Methods to account for individual differences in anatomy have been proposed including targeting based on standardized EEG electrode positions (Herwig et al., 2003b), or specific MRI coordinates (Fitzgerald et al., 2009; Herbsman et al., 2009; Rusjan et al., 2010). A randomized trial targeting anatomical coordinates chosen based on group-level DLPFC hypometabolism failed to reach its primary endpoint, but did show some clinical benefits beyond the 5 cm approach (Fitzgerald et al., 2009). Taking this approach a step further, three trials have aimed to target TMS based on individualized hypometabolic foci indentified with either SPECT (Garcia-Toro et al., 2006) or PET (Herwig et al., 2003a; Paillère Martinot et al., 2010). All three trials failed to show benefit beyond the conventional 5 cm approach.

A question relevant to the present investigation is why targeting a group-average focus of hypometaboism would be successful while targeting individualized foci would fail. Many explanations are possible, but three will be considered here. First, there may be inaccuracies in neuronavigated TMS leading to differences between the site that is targeted and the site that is actually stimulated. Further work delineating and improving this relationship will be important for any effort at individualized targeting. Second, hypometabolic foci may not be the ideal target for TMS, and perhaps some other property of the DLPFC is responsible for antidepressant response (such as connectivity to deep limbic regions). Given the anticorrelation between limbic regions and the DLPFC even in normal subjects, DLPFC hypometabolism could be secondary to limbic hyperactivity rather than causal in the disease process (Fox et al., 2012a). Finally, and most relevant to the present investigation, individual PET maps may simply be too noisy to serve as a basis for individualized targeting of TMS, and one is better off targeting a population-average focus. Critically, none of these prior trials of individualized targeting was preceded by an analysis of the reproducibility of

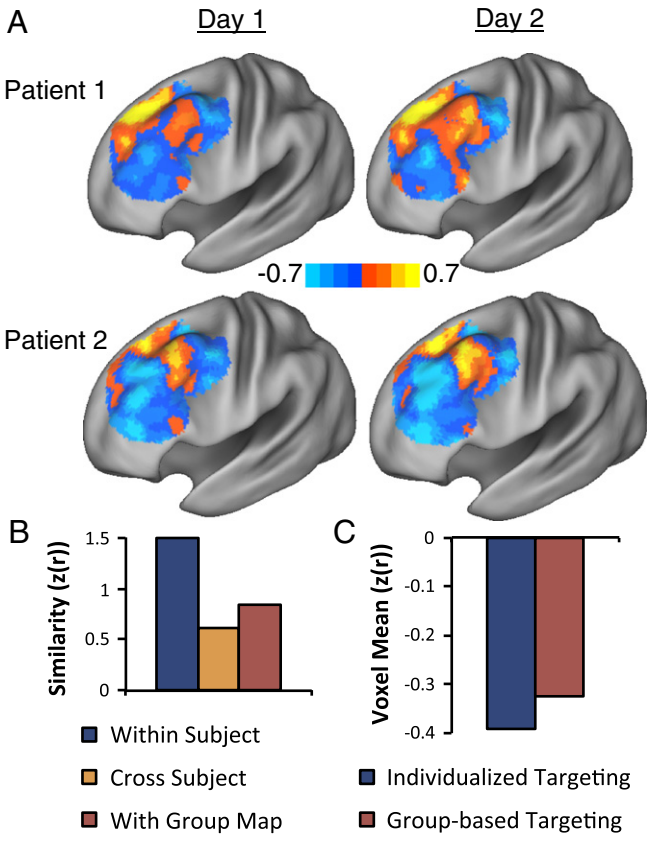

Fig. 7. Replication of primary findings in two patients with medication-refractory depression. DLPFC functional connectivity with the subgenual-based seed map is qualitatively more similar within patients scanned on two separate days (day 1 and day 2) than across patients (A). Computation of the spatial correlation coefficient confirms this qualitative impression and also shows that patients are more similar to themselves scanned on a different day than they are to the group map (B). Similar to normal subjects, selecting a TMS target (12 mm cone) based on individualized functional connectivity identifies a more anticorrelated stimulation site in an independent dataset than selecting a target based on the group map (C).

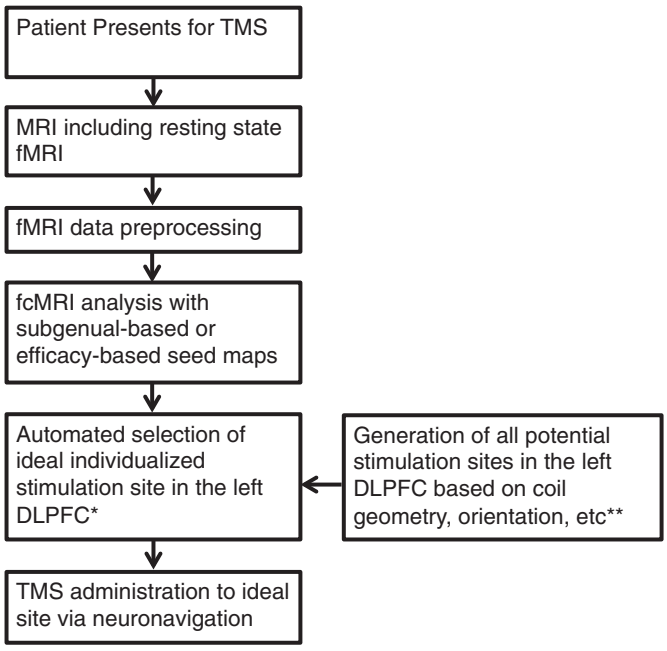

Fig. 8. Proposed strategy for individualized targeting of TMS to the left DLPFC based on resting state functional connectivity (fcMRI). *The ideal stimulation site is the volume most anticorrelated with the two seed maps. **The model of the volume of tissue activated by TMS is likely to vary depending on the particular TMS coil, stimulation intensity, coil orientation, underlying anatomy, and many other factors that could potentially be included to increase the accuracy of individualized targeting. DLPFC = dorsal lateral prefrontal cortex.

individualized hypometabolic foci or an investigation into techniques that might optimize their identification.

These pioneering trials of individualized targeting were instrumental in outlining the motivation and approach of tailoring TMS to specific patients. However, they also serve as an example of the challenges of translating a technique from application at the population level to clinical utility in individual subjects. The importance of methodological studies, such as the present work, for technique validation and optimization prior to embarking on a clinical trial should not be underestimated. Based on the results presented here, we propose an outline for individualized connectivity-based targeting of TMS that can be tested in a clinical trial (Fig. 8).

Individual differences in resting state functional connectivity MRI

Intrinsic (resting state) functional connectivity MRI is a powerful imaging technique that utilizes correlations in spontaneous fluctuations in the blood oxygenation level-dependent (BOLD) signal to assess functional relationships between regions (Biswal et al., 1995; Fox and Raichle, 2007; Van Dijk et al., 2010). This technique has several theoretical and practical advantages for clinical translation (Fox and Greicius, 2010). Accumulating evidence suggests that individual differences in intrinsic connectivity are behaviorally relevant (Baldassarre et al., 2012; Hampson et al., 2006; Koyama et al., 2011; Seeley et al., 2007; van den Heuvel et al., 2009; Zhu et al., 2011) and to some extent reproducible across scanning sessions (Braun et al., 2012; Cohen et al., 2008; Mannfolk et al., 2011; Meindl et al., 2010; Shehzad et al., 2009; Van Dijk et al., 2010; Wang et al., 2011; Zuo et al., 2010). In a recent analysis of reproducibility across 5 MRI scans over 6 months, we found that the DLPFC has some of the largest and most reproducible individual differences in functional connectivity across any area of the cortex (Mueller et al., 2012). These results complement known histological variability in this region (Rajkowska and Goldman-Rakic, 1995) and highlight the potential for individualized targeting.

Only a couple prior studies have used intrinsic connectivity to identify individualized TMS targets (Eldaief et al., 2011; Hoffman et al., 2007) (for review see (Fox et al., 2012b)). No study has focused on identification of individualized targets in the DLPFC, designed a systematized approach for TMS target selection, examined the reproducibility of these targets, or investigated factors to improve individualized targeting. These are all novel contributions of the present investigation and are critical steps towards making individualized connectivity-based guidance of TMS clinically relevant.

Using seed maps to improve signal to noise

A potentially important methodological development presented here is the use of weighted seed maps, rather than small seed regions, to improve signal to noise in single-subject connectivity analyses. If one is attempting to identify a node in the DLPFC anticorrelated with the subgenual in a specific subject, the optimal approach is not to simply perform functional connectivity with the subgenual. Rather, more reproducible results are obtained by first computing functional connectivity with the subgenual on a large independent cohort to generate a seed map. One can then subtract the area of interest from the seed map (in this case the DLPFC) then use the seed map rather than the small subgenual seed region to assess functional connectivity in the single subject. Somewhat surprisingly, the result is a better prediction of subgenual connectivity than would be obtained using the subgenual seed region itself. This approach even works

when the subgenual and surrounding medial prefrontal cortex is removed from the seed map, an important finding given the variability with which different scanners and MRI sequences sample this area of high susceptibility (Ojemann et al., 1997). Further work is needed to determine if this approach will be useful in other instances where single-subject functional connectivity with a small or noisy seed region is desired.

Impact of stimulation field size

Another important finding from the current study is the effect of modeled stimulation field size on the benefits of individualized vs population-based targeting. The smaller the modeled volume of TMS-induced activation, the more important individualized targeting becomes. This factor could become critical for more invasive and potentially focal DLPFC stimulation techniques such as epidural or subdural stimulation (Kopell et al., 2011). Conversely, individualized targeting becomes less important with larger stimulation field sizes. Given this finding, one might reasonably ask what the importance of individualized targeting might be in the current clinical setting with commercially available TMS coils. This is a difficult question to answer as it remains unclear how focal these coils truly are with respect to the volume of activated tissue. Our model of TMS-induced activation using a 12 mm radius cone suggests that individualized targeting may be relevant for current figure-eight coils, however this model was based on several assumptions (see Methods) and should be interpreted with caution. Even if the focality of current TMS coils was clearly established, it remains unclear if intense stimulation specifically focused on the most anticorrelated area of cortex or broader stimulation to a wide area of cortex with more weakly anticorrelated voxels would have a better clinical effect. In the end, there are multiple unknown variables regarding the physiological and clinical effects of TMS and true validation of the individualized connectivity-based targeting techniques presented here will require a clinical trial.

Limitations

First, the current paper is a technique development paper, not a clinical trial. These results support the potential utility of individualized targeting of TMS based on connectivity and may help enable a clinical trial, but the clinical validity of this approach remains to be proven. Second, we used highly simplified models of the tissue volume activated by TMS. More advanced models taking into account coil geometry, coil orientation, stimulation intensity, individual differences in anatomy, and probability of neuronal activation are likely to be important. Third, this paper was focused specifically on left DLPFC targets for depression. The reproducibility of individualized targets in other cortical regions or with alternate deep nuclei awaits similar validation. Finally, proof of concept was demonstrated in only two patients with medication-refractory depression. Combined with our prior results (Fox et al., 2012a), this strongly suggests that the methods presented here will be applicable in this patient population, however this awaits statistical validation in a larger patient cohort.

Conclusions

There is significant individual variability in the connectivity of the left DLPFC. This variability is stable across scanning sessions and can be used to generate individualized and reproducible TMS targets. Seed maps demonstrate more stability than a small subgenual seed region and may be an effective technique for improving signal to noise in single subject functional connectivity analyses. Finally, the more focal the stimulation field, the greater the benefit likely to come from individualized targeting. The methods presented here set the stage for a clinical trial of individualized connectivity-based targeting of left DLPFC TMS for depression. Further, these techniques might be applicable to identification of individualized targets for focal brain stimulation across a variety of disorders and stimulation techniques.

Supplementary data to this article can be found online at http://dx.doi.org/10.1016/j.neuroimage.2012.10.082.

Acknowledgments

We thank the Brain Genomics Superstruct Project for contributing data and David Alsop for assistance with MRI acquisition and sequence optimization for the depression patients. MDF was supported by NIH grant R25NS065743 and HL by NIH grant K25NS069805. APL serves on the scientific advisory boards for Nexstim, Neuronix, Starlab Neuroscience, Neuroelectrics, Neosync, and Novavision, and is listed as inventor in issued patents and patent applications on the real-time integration of transcranial magnetic stimulation (TMS) with electroencephalography (EEG) and magnetic resonance imaging (MRI). Work on this study was also supported by grants from the National Institutes of Health and National Center for Research Resources: Harvard Clinical and Translational Science Center (UL1 RR025758).

References

Ahdab, R., Ayache, S.S., Brugières, P., Goujon, C., Lefaucheur, J.-P., 2010. Comparison of "standard" and "navigated" procedures of TMS coil positioning over motor, premotor and prefrontal targets in patients with chronic pain and depression. Neurophysiol. Clin. 40, 27–36.

Baldassarre, A., Lewis, C.M., Committeri, G., Snyder, A.Z., Romani, G.L., Corbetta, M., 2012. Individual variability in functional connectivity predicts performance of a perceptual task. Proc. Natl. Acad. Sci. U. S. A. 109, 3516–3521.

Biswal, B., Yetkin, F., Haughton, V., Hyde, J., 1995. Functional connectivity in the motor cortex of resting human brain using echo-planar MRI. Magn. Reson. Med. 34, 537–541.

Braun, U., Plichta, M.M., Esslinger, C., Sauer, C., Haddad, L., Grimm, O., Mier, D., Mohnke, S., Heinz, A., Erk, S., Walter, H., Seiferth, N., Kirsch, P., Meyer-Lindenberg, A., 2012. Test-retest reliability of resting-state connectivity network characteristics using fMRI and graph theoretical measures. Neuroimage 59, 1404–1412.

Burt, T., Lisanby, S.H., Sackeim, H.A., 2002. Neuropsychiatric applications of transcranial magnetic stimulation: a meta analysis. Int. J. Neuropsychopharmacol. 5, 73–103.

Cohen, A.L., Fair, D.A., Dosenbach, N.U., Miezin, F.M., Dierker, D., Van Essen, D.C., Schlaggar, B.L., Petersen, S.E., 2008. Defining functional areas in individual human brains using resting functional connectivity MRI. Neuroimage 41, 45–57.

Deng, Z.D., Lisanby, S.H., Peterchev, A.V., 2012. Electric field depth-focality tradeoff in transcranial magnetic stimulation: Simulation comparison of 50 coil designs. Brain Stimul. (Electronic publication ahead of print).

Drevets, W.C., Bogers, W., Raichle, M.E., 2002. Functional anatomical correlates of antidepressant drug treatment assessed using PET measures of regional glucose metabolism. Eur. Neuropsychopharmacol. 12, 527–544.

Drevets, W.C., Savitz, J., Trimble, M., 2008. The subgenual anterior cingulate cortex in mood disorders. CNS Spectr. 13, 663–681.

Eldaief, M.C., Halko, M.A., Buckner, R.L., Pascual-Leone, A., 2011. Transcranial magnetic stimulation modulates the brain's intrinsic activity in a frequency-dependent manner. Proc. Natl. Acad. Sci. U. S. A. 108, 21229–21234.

Fitzgerald, P.B., Hoy, K., McQueen, S., Maller, J.J., Herring, S., Segrave, R., Bailey, M., Been, G., Kulkarni, J., Daskalakis, Z.J., 2009. A randomized trial of rTMS targeted with MRI based neuro-navigation in treatment-resistant depression. Neuropsychopharmacology 34, 1255–1262.

Fox, M.D., Greicius, M., 2010. Clinical applications of resting state functional connectivity. Front. Syst. Neurosci. 4, 19.

Fox, M.D., Raichle, M.E., 2007. Spontaneous fluctuations in brain activity observed with functional magnetic resonance imaging. Nat. Rev. Neurosci. 8, 700–711.

Fox, M.D., Snyder, A.Z., Vincent, J.L., Corbetta, M., Van Essen, D.C., Raichle, M.E., 2005. The human brain is intrinsically organized into dynamic, anticorrelated functional networks. PNAS 102, 9673–9678.

Fox, M.D., Corbetta, M., Snyder, A.Z., Vincent, J.L., Raichle, M.E., 2006. Spontaneous neuronal activity distinguishes human dorsal and ventral attention systems. PNAS 103, 10046–10051.

Fox, M.D., Buckner, R.L., White, M.P., Greicius, M.D., Pascual-Leone, A., 2012a. Efficacy of Transcranial Magnetic Stimulation Targets for Depression Is Related to Intrinsic Functional Connectivity with the Subgenual Cingulate. Biol. Psychiatry 72 (7), 595–603.

Fox, M.D., Halko, M.A., Eldaief, M.C., Pascual-Leone, A., 2012b. Measuring and manipulating brain connectivity with resting state functional connectivity magnetic resonance imaging (fcMRI) and transcranial magnetic stimulation (TMS). Neuroimage 62, 2232–2243.

Fregni, F., Pascual-Leone, A., 2007. Technology insight: noninvasive brain stimulation in neurology-perspectives on the therapeutic potential of rTMS and tDCS. Nat. Clin. Pract. Neurol. 3, 383–393.

Garcia-Toro, M., Salva, J., Daumal, J., Andres, J., Romera, M., Lafau, O., Echevarria, M., Mestre, M., Bosch, C., Collado, C., Ibarra, O., Aguirre, I., 2006. High (20-Hz) and low (1-Hz) frequency transcranial magnetic stimulation as adjuvant treatment in medication-resistant depression. Psychiatry Res. 146, 53–57.
George, M.S., Wassermann, E.M., Williams, W.A., Callahan, A., Ketter, T.A., Basser, P., Hallett, M., Post, R.M., 1995. Daily repetitive transcranial magnetic stimulation (rTMS) improves mood in depression. Neuroreport 6, 1853–1856.
Hallett, M., 2007. Transcranial magnetic stimulation: a primer. Neuron 55, 187–199.
Hampson, M., Driesen, N.R., Skudlarski, P., Gore, J.C., Constable, R.T., 2006. Brain connectivity related to working memory performance. J. Neurosci. 26, 13338–13343.
Herbsman, T., Avery, D., Ramsey, D., Holtzheimer, P., Wadjik, C., Hardaway, F., Haynor, D., George, M.S., Nahas, Z., 2009. More lateral and anterior prefrontal coil location is associated with better repetitive transcranial magnetic stimulation antidepressant response. Biol. Psychiatry 66, 509–515.
Herwig, U., Padberg, F., Unger, J., Spitzer, M., Schonfeldt-Lecuona, C., 2001. Transcranial magnetic stimulation in therapy studies: examination of the reliability of "standard" coil positioning by neuronavigation. Biol. Psychiatry 50, 58–61.
Herwig, U., Lampe, Y., Juengling, F.D., Wunderlich, A., Walter, H., Spitzer, M., Schonfeldt-Lecuona, C., 2003a. Add-on rTMS for treatment of depression: a pilot study using stereotaxic coil-navigation according to PET data. J. Psychiatr. Res. 37, 267–275.
Herwig, U., Satrapi, P., Schonfeldt-Lecuona, C., 2003b. Using the international 10–20 EEG system for positioning of transcranial magnetic stimulation. Brain Topogr. 16, 95–99.
Hoffman, R.E., Hampson, M., Wu, K., Anderson, A.W., Gore, J.C., Buchanan, R.J., Constable, R.T., Hawkins, K.A., Sahay, N., Krystal, J.H., 2007. Probing the pathophysiology of auditory/verbal hallucinations by combining functional magnetic resonance imaging and transcranial magnetic stimulation. Cereb. Cortex 17, 2733–2743.
Jenkinson, M., Bannister, P., Brady, M., Smith, S., 2002. Improved optimization for the robust and accurate linear registration and motion correction of brain images. Neuroimage 17, 825–841.
Kito, S., Fujita, K., Koga, Y., 2008. Regional cerebral blood flow changes after low-frequency transcranial magnetic stimulation of the right dorsolateral prefrontal cortex in treatment-resistant depression. Neuropsychobiology 58, 29–36.
Kito, S., Hasegawa, T., Koga, Y., 2011. Neuroanatomical correlates of therapeutic efficacy of low-frequency right prefrontal transcranial magnetic stimulation in treatment-resistant depression. Psychiatry Clin. Neurosci. 65, 175–182.
Kopell, B.H., Halverson, J., Butson, C.R., Dickinson, M., Bobholz, J., Harsch, H., Rainey, C., Kondziolka, D., Howland, R., Eskandar, E., Evans, K.C., Dougherty, D.D., 2011. Epidural cortical stimulation of the left dorsolateral prefrontal cortex for refractory major depressive disorder. Neurosurgery 69, 1015–1029 (discussion 1029).
Koyama, M.S., Di Martino, A., Zuo, X.N., Kelly, C., Mennes, M., Jutagir, D.R., Castellanos, F.X., Milham, M.P., 2011. Resting-state functional connectivity indexes reading competence in children and adults. J. Neurosci. Off. J. Soc. Neurosci. 31, 8617–8624.
Kujirai, T., Caramia, M.D., Rothwell, J.C., Day, B.L., Thompson, P.D., Ferbert, A., Wroe, S., Asselman, P., Marsden, C.D., 1993. Corticocortical inhibition in human motor cortex. J. Physiol. 471, 501–519.
Mannfolk, P., Nilsson, M., Hansson, H., Ståhlberg, F., Fransson, P., Weibull, A., Svensson, J., Wirestam, R., Olsrud, J., 2011. Can resting-state functional MRI serve as a complement to task-based mapping of sensorimotor function? A test–retest reliability study in healthy volunteers. J. Magn. Reson. Imaging 34 (3), 511–517.
Mayberg, H.S., 2009. Targeted electrode-based modulation of neural circuits for depression. J. Clin. Invest. 119, 717–725.
Mayberg, H.S., Brannan, S.K., Tekell, J.L., Silva, J.A., Mahurin, R.K., McGinnis, S., Jerabek, P.A., 2000. Regional metabolic effects of fluoxetine in major depression: serial changes and relationship to clinical response. Biol. Psychiatry 48, 830–843.
Mayberg, H.S., Lozano, A.M., Voon, V., McNeely, H.E., Seminowicz, D., Hamani, C., Schwalb, J.M., Kennedy, S.H., 2005. Deep brain stimulation for treatment-resistant depression. Neuron 45, 651–660.
Meindl, T., Teipel, S., Elmouden, R., Mueller, S., Koch, W., Dietrich, O., Coates, U., Reiser, M., Glaser, C., 2010. Test-retest reproducibility of the default-mode network in healthy individuals. Hum. Brain Mapp. 31, 237–246.
Mueller, S., Lu, J., Wang, D., Yeo, T., Sabuncu, M.R., Sepulcre, J., Fox, M.D., Li, K., Liu, H., 2012. Intra-subject and inter-subject variability of intrinsic functional connectivity. Human Brain Mapping Annual Conference.
Nahas, Z., Teneback, C., Chae, J.H., Mu, Q., Molnar, C., Kozel, F.A., Walker, J., Anderson, B., Koola, J., Kose, S., Lomarev, M., Bohning, D.E., George, M.S., 2007. Serial vagus nerve stimulation functional MRI in treatment-resistant depression. Neuropsychopharmacology 32, 1649–1660.
Ojemann, J.G., Akbudak, E., Snyder, A.Z., McKinstry, R.C., Raichle, M.E., Conturo, T.E., 1997. Anatomic localization and quantitative analysis of gradient refocused echo-planar fMRI susceptibility artifacts. Neuroimage 6, 156–167.
O'Reardon, J.P., Solvason, H.B., Janicak, P.G., Sampson, S., Isenberg, K.E., Nahas, Z., McDonald, W.M., Avery, D., Fitzgerald, P.B., Loo, C., Demitrack, M.A., George, M.S., Sackeim, H.A., 2007. Efficacy and safety of transcranial magnetic stimulation in the acute treatment of major depression: a multisite randomized controlled trial. Biol. Psychiatry 62, 1208–1216.
Padberg, F., George, M.S., 2009. Repetitive transcranial magnetic stimulation of the prefrontal cortex in depression. Exp. Neurol. 219, 2–13.
Paillère Martinot, M.-L., Galinowski, A., Ringuenet, D., Gallarda, T., Lefaucheur, J.-P., Bellivier, F., Picq, C., Bruguière, P., Mangin, J.-F., Rivière, D., Willer, J.-C., Falissard, B., Leboyer, M., Olié, J.-P., Artiges, E., Martinot, J.-L., 2010. Influence of prefrontal target region on the efficacy of repetitive transcranial magnetic stimulation in patients with medication-resistant depression: a [(18)F]-fluorodeoxyglucose PET and MRI study. Int. J. Neuropsychopharmacol. 13, 45–59.
Pascual-Leone, A., Rubio, B., Pallardo, F., Catala, M.D., 1996. Rapid-rate transcranial magnetic stimulation of left dorsolateral prefrontal cortex in drug-resistant depression. Lancet 348, 233–237.
Pascual-Leone, A., Davey, N.J., Rothwell, J., Wassermann, E.M., Puri, B.K., 2002. Handbook of Transcranial Magnetic Stimulation. Arnold Oxford University Press distributor, London.
Rajkowska, G., Goldman-Rakic, P.S., 1995. Cytoarchitectonic definition of prefrontal areas in the normal human cortex: II. Variability in locations of areas 9 and 46 and relationship to the Talairach Coordinate System. Cereb. Cortex 5, 323–337.
Rusjan, P.M., Barr, M.S., Farzan, F., Arenovich, T., Maller, J.J., Fitzgerald, P.B., Daskalakis, Z.J., 2010. Optimal transcranial magnetic stimulation coil placement for targeting the dorsolateral prefrontal cortex using novel magnetic resonance image-guided neuronavigation. Hum. Brain Mapp. 31, 1643–1652.
Seeley, W.W., Menon, V., Schatzberg, A.F., Keller, J., Glover, G.H., Kenna, H., Reiss, A.L., Greicius, M.D., 2007. Dissociable intrinsic connectivity networks for salience processing and executive control. J. Neurosci. 27, 2349–2356.
Shehzad, Z., Kelly, A.M., Reiss, P.T., Gee, D.G., Gotimer, K., Uddin, L.Q., Lee, S.H., Margulies, D.S., Roy, A.K., Biswal, B.B., Petkova, E., Castellanos, F.X., Milham, M.P., 2009. The resting brain: unconstrained yet reliable. Cereb. Cortex 19, 2209–2229.
Talairach, J., Tournoux, P., 1988. Co-Planar Stereotaxic Atlas of the Human Brain. Thieme Medical Publishers, Inc., New York.
Thielscher, A., Kammer, T., 2004. Electric field properties of two commercial figure-8 coils in TMS: calculation of focality and efficiency. Clin. Neurophysiol. 115, 1697–1708.
Valero-Cabre, A., Payne, B.R., Rushmore, J., Lomber, S.G., Pascual-Leone, A., 2005. Impact of repetitive transcranial magnetic stimulation of the parietal cortex on metabolic brain activity: a 14C-2DG tracing study in the cat. Exp. Brain Res. 163, 1–12.
van den Heuvel, M.P., Stam, C.J., Kahn, R.S., Hulshoff Pol, H.E., 2009. Efficiency of functional brain networks and intellectual performance. J. Neurosci. 29, 7619–7624.
van der Kouwe, A.J., Benner, T., Salat, D.H., Fischl, B., 2008. Brain morphometry with multiecho MPRAGE. Neuroimage 40, 559–569.
Van Dijk, K.R., Hedden, T., Venkataraman, A., Evans, K.C., Lazar, S.W., Buckner, R.L., 2010. Intrinsic functional connectivity as a tool for human connectomics: theory, properties, and optimization. J. Neurophysiol. 103, 297–321.
Van Dijk, K.R., Sabuncu, M.R., Buckner, R.L., 2012. The influence of head motion on intrinsic functional connectivity MRI. Neuroimage 59, 431–438.
Van Essen, D.C., 2005. A population-average, landmark- and surface-based (PALS) atlas of human cerebral cortex. Neuroimage 28, 635–662.
Wagner, T., Valero-Cabre, A., Pascual-Leone, A., 2007. Noninvasive human brain stimulation. Annu. Rev. Biomed. Eng. 9, 527–565.
Wang, J.-H., Zuo, X.-N., Gohel, S., Milham, M.P., Biswal, B.B., He, Y., 2011. Graph theoretical analysis of functional brain networks: test–retest evaluation on short- and long-term resting-state functional MRI data. PLoS One 6, e21976.
Wu, J., Buchsbaum, M.S., Gillin, J.C., Tang, C., Cadwell, S., Wiegand, M., Najafi, A., Klein, E., Hazen, K., Bunney Jr., W.E., Fallon, J.H., Keator, D., 1999. Prediction of antidepressant effects of sleep deprivation by metabolic rates in the ventral anterior cingulate and medial prefrontal cortex. Am. J. Psychiatry 156, 1149–1158.
Yeo, B.T., Krienen, F.M., Sepulcre, J., Sabuncu, M.R., Lashkari, D., Hollinshead, M., Roffman, J.L., Smoller, J.W., Zollei, L., Polimeni, J.R., Fischl, B., Liu, H., Buckner, R.L., 2011. The organization of the human cerebral cortex estimated by functional connectivity. J. Neurophysiol. 106 (3), 1125–1165.
Zhu, Q., Zhang, J., Luo, Y.L., Dilks, D.D., Liu, J., 2011. Resting-state neural activity across face-selective cortical regions is behaviorally relevant. J. Neurosci. 31, 10323–10330.
Zuo, X.-N., Kelly, C., Adelstein, J.S., Klein, D.F., Castellanos, F.X., Milham, M.P., 2010. Reliable intrinsic connectivity networks: test–retest evaluation using ICA and dual regression approach. Neuroimage 49, 2163–2177.